

## Research Article

# Spin Polarization and Exchange Interaction in a Diluted Magnetic Quantum Dot

A. John Peter<sup>1</sup> and K. Lily Mary Eucharista<sup>2</sup>

<sup>1</sup> Government Arts College, Melur, Madurai-625 106, India

<sup>2</sup> Arul Anandar College, Karumathur, Madurai-625 514, India

Correspondence should be addressed to A. John Peter, a.johnpeter@rediffmail.com

Received 15 October 2008; Revised 20 February 2009; Accepted 1 April 2009

Recommended by Joseph Poon

The spin interaction energy of different  $\text{Mn}^{2+}$  ions with and without an itinerant electron is evaluated for different dot radii. Magnetization is calculated for various concentrations of  $\text{Mn}^{2+}$  ions with different dot sizes. Spin polaronic shifts are estimated using a mean field theory. The lowest binding energies of electrons in a  $\text{Cd}_{1-x}\text{Mn}_x\text{Te}$  quantum dot are also calculated. Results are obtained for  $\text{Cd}_{1-x_{\text{in}}}\text{Mn}_{x_{\text{in}}}\text{Te}/\text{Cd}_{1-x_{\text{out}}}\text{Mn}_{x_{\text{out}}}\text{Te}$  structures as a function of the dot radius variationally. It is found that (i) more number of  $\text{Mn}^{2+}$  spins enhance the spin polaronic effect and it varies linearly with the concentration, (ii) spin polarization of  $\text{Mn}^{2+}$  ions increases with the concentration for any dot radii, (iii) the magnetization of Mn subsystem increases with the concentration of  $\text{Mn}^{2+}$  ions and this feature is predominant for smaller dots, and (iv) variation of increase in ionization energy is sharper for smaller dots with increase in concentration. These results are discussed with the available data in literature.

Copyright © 2009 A. J. Peter and K. L. M. Eucharista. This is an open access article distributed under the Creative Commons Attribution License, which permits unrestricted use, distribution, and reproduction in any medium, provided the original work is properly cited.

## 1. Introduction

Recent advances in nanofabrication technology have allowed the construction of structures with lower dimensions. The most recent achievement is the fabrication of zero-dimension quantum structures, usually called quantum dots. Due to their small size these structures exhibit physical properties that are quite different from those of the bulk semiconductor constituents. It is expected that these properties will show more pronounced differences as the confinement is increased with the lowering of the dimensionality. More specifically, the shape and the size of the nanostructure have a strong influence on the optical properties [1].

Diluted magnetic semiconductors (DMSs) are expected to play an important role in interdisciplinary materials science and future electronics because charge and spin degrees of freedom accommodated into a single material exhibit interesting magnetic, magneto-optical, magnetoelectronic, and other properties [2]. Controlling the spin state of electrons provides an important versatility for future nanoelectronics [3]. Most of the envisioned spintronic devices are based on spin transfer mechanisms on the nanoscale.

For this purpose, new materials have been synthesized with highly spin polarized bands, and novel experimental techniques are being applied to characterize the spin state of the charge carriers [4–6]. The range, strength, and sign of exchange interactions between magnetic impurities in DMSs depend on the density and nature of the states at the Fermi level. Mn-doped semiconductors of the families (II,Mn)–VI and (III,Mn)–V order ferromagnetically in the presence of carriers that mediate indirect exchange interactions between Mn. (III,Mn)V DMSs are promising spintronic materials with high spin polarization of bound magnetic polarons [7–9] and with a wide variety of spin-dependent transport properties [10]. While considerable effort is concentrated to enhance the ferromagnetic transition temperature [11, 12]. Smith et al., [13] showed the evidence of exciton magnetic polarons in CdMnTe QDs form through the spontaneous ferromagnetic alignment of the Mn.

Study of DMSs and their heterostructures have centered mostly on II–VI semiconductors, such as CdTe and ZnSe, in which the valence of the cations matches that of the common magnetic ions such as Mn. Although this phenomenon makes these DMSs relatively easy to prepare in bulk form

as well as in thin epitaxial layers, II–VI-based DMSs have been difficult to dope to create p and n-type, which made the material less attractive for applications. Moreover, the magnetic interaction in II–VI DMSs is dominated by the antiferromagnetic exchange among the Mn spins, which results in the paramagnetic, antiferromagnetic, or spin glass behavior of the material. It was not possible until very recently to make a II–VI DMS ferromagnetic at low temperature in modulation-doped QW structures exploiting RKKY mechanism [14].

Diluted magnetic semiconductors (DMSs) are compound of alloy semiconductors containing a large fraction of magnetic ions ( $\text{Mn}^{2+}$ ,  $\text{Cr}^{2+}$ ,  $\text{Fe}^{2+}$ ,  $\text{Co}^{2+}$ ) and are studied mainly on II–VI-based materials such as CdTe and ZnSe. This is because such +2 magnetic ions are easily incorporated into the host II–VI crystals by replacing group II cations. In such II–VI-based DMSs such as  $(\text{CdMn})\text{Te}$ ,  $(\text{CdMn})\text{Se}$ , magneto-optic properties were extensively studied, and optical isolators were recently fabricated using their large Faraday effect [15]. Also, recently, a controllable fabrication of dots with only a single Mn ion and the photoluminescence studies distinguishing various positions of such Mn ion or anisotropy in the quantum confinement and the temperature of the onset of magnetization in DMS QDs higher than in the bulk DMSs have been studied [16, 17]. Moreover, the carrier-mediated ferromagnetism bulk DMS such as light- and bias-controlled ferromagnetism have also been studied. The interaction among these spins leads to ferromagnetic order at low temperatures, which is not only to create spin-polarized carriers but also optical or electrical injection can create highly spin-polarized carrier density even in nonmagnetic semiconductors [18]. Petukhov et al. [19], have proposed a model of carrier-mediated ferromagnetism in semiconductors accounting for the temperature dependence of the carriers. Their model permits analysis of the thermodynamic stability of competing magnetic states, opening the door to the construction of magnetic phase diagrams. The complete details of properties of DMS material have been reviewed by Furdyna [20]. Optically detected cyclotron resonance of two-dimensional electrons has been studied in nominally undoped CdTe/(Cd,Mn)Te quantum wells [21] where they studied an increase of the electron cyclotron mass from  $0.099 m_0$  to  $0.112 m_0$  with well width decreasing from 30 down to 3.6 nm. Diluted magnetic oxide semiconductors are considered to be one of the strong candidates to realize room temperature ferromagnetism. Among them, Mn-doped ZnO can be regarded as a class of Mn-doped II–VI semiconductors, and the properties are similar to the typical II–VI magnetic semiconductors [22, 23].

In this work, the lowest binding energy of the donor electron in a diluted magnetic semiconductor of a  $\text{Cd}_{1-x}\text{Mn}_x\text{Te}$  quantum dot is calculated. We investigate theoretically the donor bound spin polaronic effect in a quantum dot. The mean field theory with modified Brillouin function that is already used for bulk and quantum well cases has been extended to the case of a QD, and we estimate the spin polaronic shifts to the impurity ionization energies. Moreover, the introduction of magnetic ions such as Mn into these compounds leads to the formation of diluted magnetic

semiconductors, in which the exchange interaction between the magnetic ions and electronic states opens perspectives for interesting new phenomena. One such possibility is observing a situation in which the exchange-interaction-enhanced spin splitting of a Landau level coinciding with the energy separation between adjacent Landau levels (cyclotron energy), where interaction of the two resonances might be expected. Donor ionization energy and the spin interaction energy are calculated with different concentrations of  $\text{Mn}^{2+}$  ions for different dot radii. The spin interaction energy of among  $\text{Mn}^{2+}$  ions is evaluated for different dot radii. Magnetization is calculated for various concentrations with the dot sizes.

We would like to point out that the lowest binding energy and the impurity binding are calculated for a  $\text{Cd}_{1-x}\text{Mn}_x\text{Te}$ , within the single band approximation, varying the variational parameter. The magnetization is computed using the variational parameter with the impurity concentration. The donor electron in a doped semimagnetic semiconductor has a huge orbit ( $\sim 50 \text{ \AA}$ ) in which there occur several manganese ions which are polarized due to the spin of the carrier which is an exchange mechanism resulting the concept of Bound Magnetic Polaron (BMP). The spin polaronic effect is also computed with the same variational parameter and the wave function, and it is estimated with the mean field approximation using modified Brillouin function.

## 2. Model and Calculations

**2.1. Ionization Energy.** Our system consists of a spherical dot (depth  $V$ , and radius  $R$ ) containing a donor impurity inside the QD of the magnetically nonuniform “spin-doping” superlattice system such as  $\text{Cd}_{1-x_{\text{in}}}\text{Mn}_{x_{\text{in}}}\text{Te}/\text{Cd}_{1-x_{\text{out}}}\text{Mn}_{x_{\text{out}}}\text{Te}$  with different concentrations of  $x_{\text{in}}$  and  $x_{\text{out}}$  of Mn ions in- and outside the QD. Such a QD may be fabricated by the method of evolution of self-assembled quantum dots (QDs) in the Stransky-Krastanow mode as in the case of  $\text{Cd}_{1-x_{\text{in}}}\text{Mn}_{x_{\text{in}}}\text{Se}$  QDs or by electron beam lithography and wet chemical etching which is used to fabricate quantum wires [24].

The system is described by the following Hamiltonian:

$$H = H_e + g\mu_B s_z B - J_{s-d} \sum_I \bar{S}_I \cdot \bar{s} \delta(\bar{r} - \bar{R}_I). \quad (1)$$

Let us analyze the three terms contributing to  $H$ .  $H_e$  is the part of Hamiltonian which describes the itinerant electron. The second term is the Zeeman coupling between localized spins and an external magnetic field  $B$  where  $\mu_B$  is the Bohr magneton. And the third term is the magnetic Hamiltonian for one itinerant electron with spin  $\bar{s}$  located at  $\bar{r}$  and one Mn ion with  $\bar{S}$  located at  $\bar{R}$ . In the presence of hydrogenic impurity, the Hamiltonian is the sum of kinetic energy and potential energy, given by

$$H_e = -\frac{\hbar^2}{2m^*} \nabla^2 - \frac{e^2}{\epsilon_0 r} + V(r), \quad (2)$$

where  $m^*$  is the effective mass, and  $\epsilon_0$  is the static dielectric constant of CdTe. By introducing the effective Rydberg  $R_y^*$ ,

as the unit of energy and the effective Bohr radius ( $60 \text{ \AA}$ ) as the length unit, the Hamiltonian given in (2) becomes

$$H_e = -\nabla^2 - \frac{2}{r} + \frac{V(r)}{R_y^*}. \quad (3)$$

The lowest state energies are obtained using the wave function

$$\psi = \begin{cases} N_2 \frac{\sin k_1 r}{r}, & r \leq R, \\ N_3 \exp(-k_2 r), & r > R, \end{cases} \quad (4)$$

where  $N_2, N_3$  are normalization constants,  $k_1 = (2m^*E/\hbar^2)^{1/2}$ , and  $k_2 = (2m^*(E-V)/\hbar^2)^{1/2}$ . For a finite barrier case we choose  $x = 0.02$ ; hence  $V = 29.92R_y^*$ .

With the inclusion of the impurity potential in the Hamiltonian forces to use of the variational approach. Then the trial wave function for the ground state with the impurity present is taken as

$$\psi = \begin{cases} N_4 \frac{\sin k_1 r}{r} \exp(-\alpha_1 r), & r \leq R, \\ N_5 \exp(-k_2 r) \exp(-\alpha_1 r), & r > R, \end{cases} \quad (5)$$

where  $\alpha_1$  is the variational parameter, and  $N_4, N_5$  are normalization constants.

The ionization energy is given by

$$E_{\text{ion}} = E_{\text{sub}} - \langle H \rangle_{\text{min}}, \quad (6)$$

where  $E_{\text{sub}}$  is the lowest subband energy obtained with the impurity. Thus the ionization energy is obtained, varying  $\alpha_1$  for different dot sizes with different concentrations of Mn ions.

The  $H_{\text{zee}}$  term is given by

$$H_{\text{zee}} = g\mu_B s_z B = xJ_{s-d} s_z \langle S_z \rangle, \quad (7)$$

which is the Zeeman coupling between localized spins and an external magnetic field  $B$ . Direct interactions between the magnetic moments of Mn ions are much smaller than the interaction with the carrier spins [25], and also for an electron spin, the separation between the Zeeman levels is given by  $\hbar\omega = \hbar\gamma B_0$  where  $\gamma$  is the gyromagnetic ratio. For  $B_0 \sim 40$  Tesla, we obtain a value of  $\sim 5$  meV for the separation. As this is small when compared to the exchange energy, we drop the Zeeman Effect. Equation (7) is the antiferromagnetic exchange interaction arising between the spin of a conduction electron and the  $\text{Mn}^{2+}$  spins. Here  $S_I$  is the spin of the  $\text{Mn}^{2+}$  ion at position  $R_I$ , and  $s$  is the spin of the conduction electron centered at  $r$ . The exchange interaction  $J(r, R_I)$  is dependent on the overlap between the orbital of the conduction electron and of the 3d electrons.

**2.2. Spin Polaronic Effect.** Kasuya and Yanase [26], who explained the transport properties of magnetic semiconductors, originally developed the theory of spin polaron (SP). This mean field theory, which invokes the exchange interaction between the carrier and magnetic impurity in

the presence of an external magnetic field  $B$ , yields the spin polaronic shift,  $E_{\text{sp}}$ , with the modified Brillouin function [27]:

$$E_{\text{sp}} = \frac{1}{2} \alpha N_0 \int x S_0(x) |\psi|^2 B_s \left[ \frac{S\alpha |\psi|^2}{2k_B [T + T_0(x)]} \right] d\tau, \quad (8)$$

where  $\alpha$  is the exchange coupling parameter,  $S$  is the  $\text{Mn}^{2+}$  spin, and  $xN_0$  is the Mn ion concentration. The integration is on spatial coordinates. Also  $g \approx 2, S_0(x)$ , the effective spin, and  $T_0(x)$ , the effective temperature, are the semi-phenomenological parameters, which describe the paramagnetic response of the  $\text{Mn}^{2+}$  ions in the bulk  $\text{Cd}_{1-x}\text{Mn}_x\text{Te}$  [28],  $k_B$  is the Boltzmann constant, and  $B_s(\eta)$  is the modified Brillouin function. In (8),  $\psi$  is the envelope function given by (5).

The parameters used in our calculations are  $N_0 = 2.94 \times 10^{22} \text{ cm}^{-3}$ ,  $\alpha N_0 \approx 220$  meV, and the semi-phenomenological parameters  $S_0(X_{\text{in}} = 0.02) = 1.97$ ,  $T_0(X_{\text{in}} = 0.02) = 0.94$ , [29]. The lattice constant is around  $6.48 \text{ \AA}$ . We estimate  $N_0$ , the atomic concentration of Cd, to be  $2.940 \times 10^{22} \text{ cm}^{-3}$ . For  $x = 0.01$  in  $\text{Cd}_{1-x_{\text{out}}}\text{Mn}_{x_{\text{out}}}\text{Te}$  barrier, there are about 134  $\text{Mn}^{2+}$  ions in a volume  $4\pi a^{*3}/3$ .

Using the envelop function given in (4) with the appropriate variational parameters, we obtain

$$E_{\text{sp}} = \frac{1}{2} \alpha N_0 [X_{\text{in}} S_0(X_{\text{in}}) I_1 + X_{\text{out}} S_0(X_{\text{out}}) I_2], \quad (9)$$

where

$$I_1 = \int |\psi_{\text{in}}|^2 B_s(\eta_1) d\tau, \quad I_2 = \int |\psi_{\text{out}}|^2 B_s(\eta_2) d\tau, \\ B_s(\eta_j) = \frac{2S+1}{2S} \coth\left(\frac{2S+1}{2S} \eta_j\right) - \frac{1}{2S} \coth\left(\frac{\eta_j}{2S}\right), \quad (10)$$

with  $\eta_1 = S\alpha |\psi_{\text{in}}|^2 / 2k_B [T + T_0(x_{\text{in}})]$  and  $\eta_2 = S\alpha |\psi_{\text{out}}|^2 / 2k_B [T + T_0(x_{\text{out}})]$ .

The factor  $B_s(\eta_j)$  represents the spin polarization of the  $\text{Mn}^{2+}$  cations. The spin of the  $\text{Mn}^{2+}$  cation is  $S = 5/2$ .  $B_s(\eta_j)$  is the standard Brillouin function. Such a simplified Brillouin-function approach is quite common when dealing with quasi-low dimensional systems.

**2.3. Spin Exchange-Interaction Energy.** The magnetization of the magnetic ions competes with spin-orbit coupling [30, 31]:

$$\xi = \frac{g_{\text{Mn}} \mu_B S B - J_{s-d} S (n_{\text{down}} - n_{\text{up}}) / 2}{k_B T}, \quad (11)$$

where  $\mu_B$  is the Bohr magneton,  $g_{\text{Mn}}$  is the  $g$  factor of Mn ions, and  $n_{\text{down}}$  and  $n_{\text{up}}$  are the spin-down and spin-up concentrations measured for a particular dot radius. The first term in the numerator of (11) represents the contribution of the Zeeman coupling between the localized spin and the magnetic field. The second term in the numerator of (11) (sometimes called ‘‘feedback mechanism’’) represents

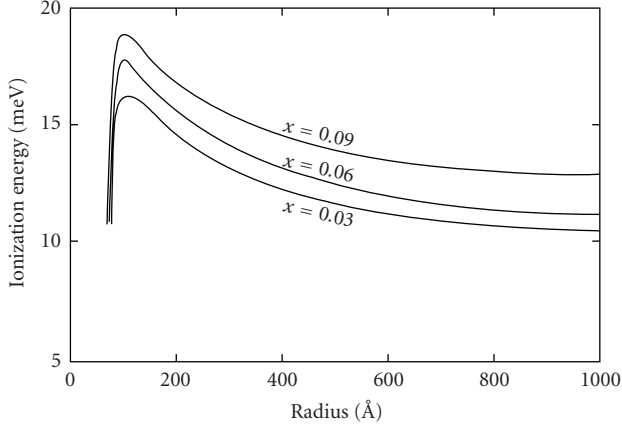


FIGURE 1: Variation of ionization energy with dot size for different concentrations of Mn ions in a  $\text{Cd}_{1-x}\text{Mn}_x\text{Te}$  QD.

the kinetic exchange contribution which, in principle, can induce spontaneous spin-polarization, that is, in the absence of an external magnetic field. Choosing the cell dimension in CdTe to be  $6.48\text{\AA}$ , taking 8 atoms per unit cell we have calculated the total number of ions present in a spherical quantum dot for different concentrations. Thus the spin exchange interaction energy among Mn ions is obtained for two different dot radii as shown in Figure 4.

**2.4. Magnetization Energy.** Following formalism describes the magnetization energy in the CdMnTe dot. Intending to consider semimagnetic semiconductors  $\text{Cd}_{1-x}\text{Mn}_x\text{Te}$  we will incorporate into the Hamiltonian the exchange Heisenberg interaction of the conduction band electrons with Mn ions. We consider the magnetic Hamiltonian for one itinerant electron with spin  $\bar{s}$  located at  $\bar{r}$  and one Mn ions with  $S_n^{\text{Mn}}$  located at  $R_n$  as

$$H_m = - \sum_n J_{sd}(r - R_n) S_n^{\text{Mn}} s, \quad (12)$$

where  $J_{s-d}$  is the coupling strength due to the spin-spin exchange interaction between the d electrons of the  $\text{Mn}^{2+}$  cations and the s- or p-band electrons; it is negative for conduction band electrons and the sum runs over all the Mn ions. The value of  $J_{sd}$  is taken as  $12 \times 10^{-3} \text{ eVnm}^3$ . We will use the mean-field approximation inserting the mean value of Mn spin in z direction. In the mean field approximation,  $H^e \rightarrow H_{\text{Mn}}^e \equiv g_e \mu_B \bar{s} \cdot \bar{h}^e$  and  $H^{\text{Mn}} \rightarrow H_{\text{MF}}^{\text{Mn}} \equiv g_{\text{Mn}} \mu_B \bar{s} \cdot \bar{h}^{\text{Mn}}$ , where  $g_{\text{Mn}} = 2$ ,  $\mu_B$  is the Bohr magneton,  $S = 5/2$  is the spin of a manganese atom, and  $h^e$  and  $h^{\text{Mn}}$  are the effective magnetic fields acting upon electrons and magnetic impurities, respectively, and can be given as

$$\begin{aligned} h^e &= \frac{1}{g_e \mu_B} J_{sd} N_{\text{Mn}} \langle S_z \rangle, \\ h^{\text{Mn}} &= \frac{1}{g_e \mu_B} J_{sd} M^e. \end{aligned} \quad (13)$$

Here,  $N_{\text{Mn}} = 4x/a_0^3$  is the density of Mn ions with  $a_0^3$  being the unit cell volume.  $M^e = \sum_n J_{sd}(s) \delta(r - R_n)$  is

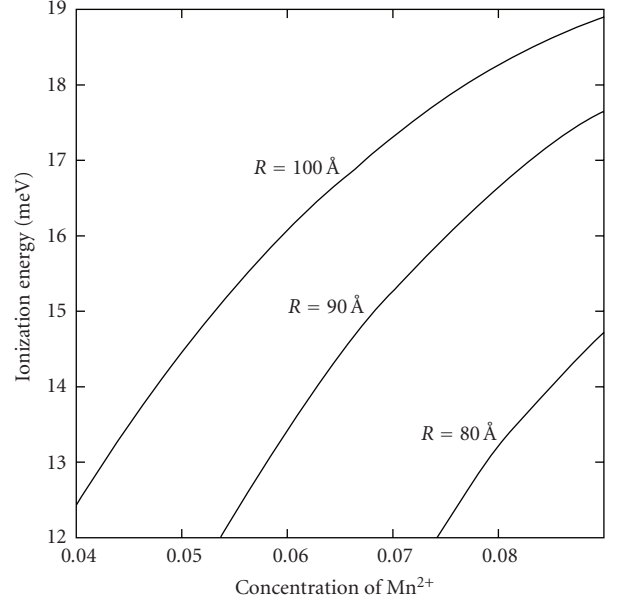


FIGURE 2: Variation of ionization energy with concentration of Mn ions for different sizes of dot of  $\text{Cd}_{1-x}\text{Mn}_x\text{Te}$ .

the magnetization density of the electron subsystem which is assumed to be uniform within the length scale of the magnetic interactions; so the magnetic response of the Fermi sea electrons to the field  $h^e$  is given by

$$M^e = g_e \mu_B s^2 D^e(E_F) h^e, \quad (14)$$

where the density of states of electron gas with the effective mass and the electron concentration  $n$  is

$$D^e(E_F) = (3\pi^2)^{-2/3} (3m^*/\hbar^2) n^{1/3}. \quad (15)$$

On the other hand, the magnetic response of the impurity spin to the effective field  $h^{\text{Mn}}$  is given by

$$M^{\text{Mn}} = g_{\text{Mn}} \mu_B N_{\text{Mn}} \langle S_z \rangle = g_{\text{Mn}} \mu_B N_{\text{Mn}} S B_s \left( \frac{g_{\text{Mn}} \mu_B N_{\text{Mn}} S h^{\text{Mn}}}{k_B T} \right), \quad (16)$$

where  $B_s(x)$  is given as (10). So within the spirit of a mean field framework the magnetization of Mn subsystem is the given by

$$M^{\text{Mn}} = g_{\text{Mn}} \mu_B N_{\text{Mn}} S B_s \left( \frac{J_{sd} S}{2k_B T} M^e \right), \quad (17)$$

which should be determined self consistently with the electron magnetization:

$$M^e = \frac{J_{sd} D^e(E_F)}{g_{\text{Mn}} \mu_B} M^{\text{Mn}}. \quad (18)$$

### 3. Results and Discussion

The donor binding energy as a function of dot radius different concentrations of Mn ions is given in Figure 1.

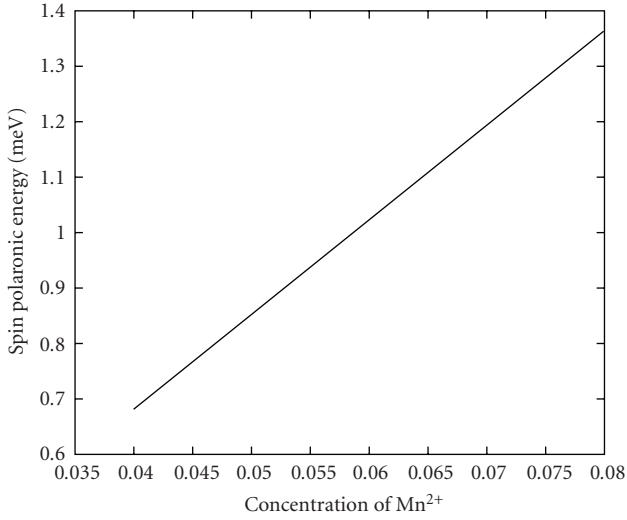


FIGURE 3: Variation of spin polaronic energy with concentration of Mn ions for the dot size of 100 Å.

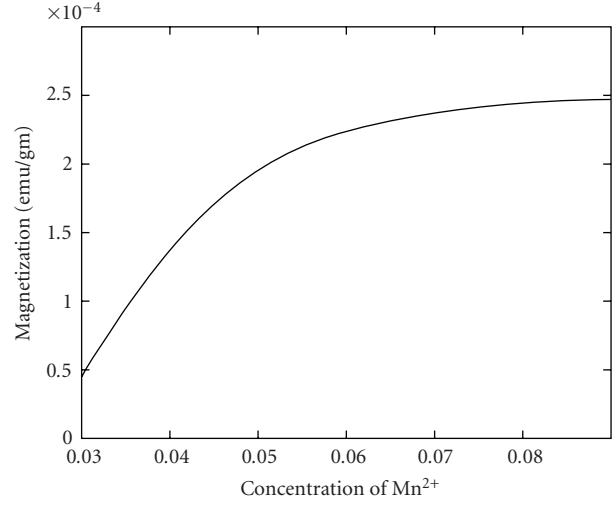


FIGURE 5: Variation of magnetization with different concentrations of Mn ions in a Cd<sub>1-x</sub>Mn<sub>x</sub>Te QD with a finite barrier height.

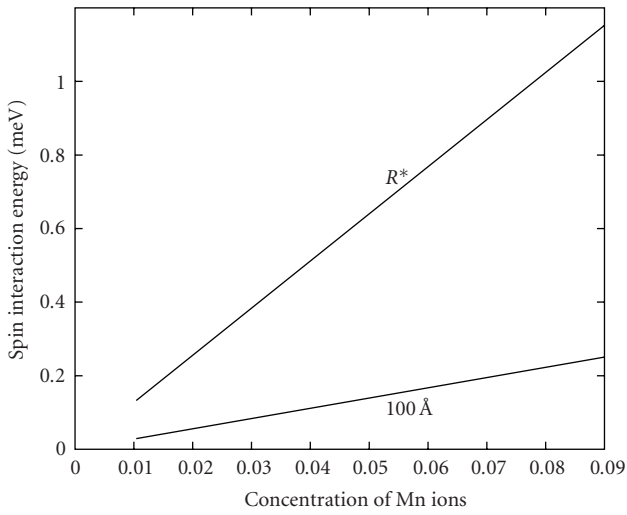


FIGURE 4: Variation of spin interaction energy with concentration of Mn ions for two different dot sizes of Cd<sub>1-x</sub>Mn<sub>x</sub>Te QD. R\* = 60.08 Å. The spin interaction energy has been calculated using (11) for different concentrations.

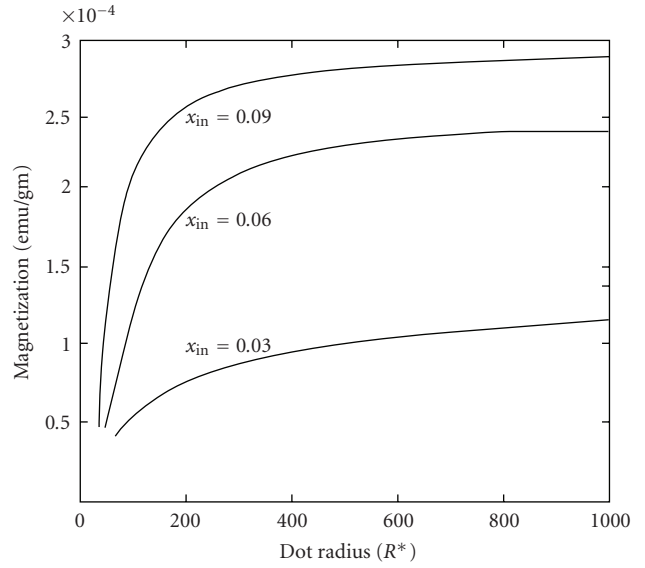


FIGURE 6: Variation of magnetization with dot radius for different concentrations of Mn ions in a Cd<sub>1-x<sub>in</sub></sub>Mn<sub>x<sub>in</sub></sub>Te/Cd<sub>1-x<sub>out</sub></sub>Mn<sub>x<sub>out</sub></sub>Te QD.

As expected, the binding energy decreases with an increase of dot radius, reaching the bulk value for larger dot radii. As the dot radius approaches zero, the confinement becomes negligibly small, and in the finite barrier problem the tunneling becomes huge. The binding energy again approaches the bulk value of the barrier. In all the cases, the ionization energy approaches the bulk value in both the limits of  $L \rightarrow 0$  and  $L \rightarrow \infty$  corresponding to one effective Bohr radius of CdTe, 11.38 meV, which is the ionization energy of the donor for the bulk. Hence the variation of ionization energy with dot radius shows a peak around  $1.5R^*$  for all the concentrations. This is a well-known result in all quantum well structures [32]. Donor ionization

energy becomes higher with the concentration for any dot radii.

Figure 2 represents the variation of ionization energies of a donor impurity with concentration of Mn ions for three different dot radii. It is clear that donor ionization energy increases with the concentration. For larger dot radii, the ionization energy increases slowly with the increase of concentration whereas the variation of increase in ionization energy is sharper for smaller dots due to the confinement. These results are very good agreement with the other investigators qualitatively [33, 34]. The slope measures with the values of  $133 \text{ meV}/\text{Å}^3$  for  $= 100 \text{ Å}$ ,  $125 \text{ meV}/\text{Å}^3$  for  $90 \text{ Å}$  and  $111 \text{ meV}/\text{Å}^3$  for  $80 \text{ Å}$ .

In Figure 3, we have plotted the variation of spin polaronic energy with concentration of Mn ions for the dot size of  $100 \text{ \AA}$ . The spin polarization energy increases with the concentration of Mn ions. This variation is found to be linearly varying. Our results are closely in agreement with the results of Kai Chang et al. [30], who have found the energy dispersion of an electron in a double quantum wire with a diluted magnetic semiconductor barrier recently.

Figure 4 shows the variation of spin interaction energy among Mn ions with for two different dot sizes of  $\text{Cd}_{1-x}\text{Mn}_x\text{Te}$  QD. In both cases the spin exchange interaction energy of confined electrons increases with the concentrations linearly. The variation of spin correlation energy is sharper when the radius of the dot is higher whereas there occurs a slow variation for smaller dot radii.

In Figure 5, we have plotted for the variation of magnetization with different concentrations of Mn ions in a  $\text{Cd}_{1-x_{\text{in}}}\text{Mn}_{x_{\text{in}}}\text{Te}/\text{Cd}_{1-x_{\text{out}}}\text{Mn}_{x_{\text{out}}}\text{Te}$  QD. As the concentration of Mn ions increases, the magnetization of Mn subsystem also increases. This mechanism has clearly brought out in Figure 6 which has been plotted for variation of magnetization with dot radius for different concentrations of Mn ions in a  $\text{Cd}_{1-x_{\text{in}}}\text{Mn}_{x_{\text{in}}}\text{Te}/\text{Cd}_{1-x_{\text{out}}}\text{Mn}_{x_{\text{out}}}\text{Te}$  in a finite barrier model. Magnetization decreases when dot radius increases for all the concentrations of Mn ions. As concentration increases, the magnetization also increases for all the dot radii whereas these changes occur appreciably for smaller dots. Magnetization is stronger for smaller dots with high concentration as expected. Magnetization is almost constant for larger dot radii for any concentration of Mn ions [35]. Magnetization of the magnetic ions competes with spin-orbit coupling, and the effects of the spin-subband populations and the spin-polarization as functions of the temperature,  $T$ , and the in-plane magnetic field,  $B$ , for narrow to wide dilute-magnetic-semiconductor quantum wells have been studied recently [35].

In conclusion, the spin polarization energy of a confined donor electron has been studied for different concentrations of Mn ions for the finite dot of  $\text{Cd}_{1-x}\text{Mn}_x\text{Te}$ . The magnetization of Mn subsystems and the strength of spin exchange energy of confined electrons have been discussed. The main results are the spin polaronic effect raises the binding energy, but this feature predominantly occurs only for smaller dots, the variation of increase in ionization energy is sharper for smaller dots due to the confinement, and the spin interaction energy increases with the concentration of Mn ions having a sharp variation for larger dots. However, this problem may be improved in the line of thought of considering spin polarization energy self consistently which requires a lot of computation techniques. Experimental efforts are encouraged to lend support to our calculations.

## References

- [1] S. Baskoutas, "Excitons and charged excitons in InAs nanorods," *Chemical Physics Letters*, vol. 404, no. 1–3, pp. 107–111, 2005.
- [2] T. Mizokawa, T. Nambu, A. Fujimori, T. Fukumura, and M. Kawasaki, "Electronic structure of the oxide-diluted magnetic semiconductor  $\text{Zn}_{1-x}\text{Mn}_x\text{O}$ ," *Physical Review B*, vol. 65, no. 8, Article ID 085209, 5 pages, 2002.
- [3] D. D. Awschalom and M. E. Flatté, "Challenges for semiconductor spintronics," *Nature Physics*, vol. 3, no. 3, pp. 153–159, 2007.
- [4] R. J. Soulen Jr., J. M. Byers, M. S. Osofsky, et al., "Measuring the spin polarization of a metal with a superconducting point contact," *Science*, vol. 282, no. 5386, pp. 85–88, 1998.
- [5] S. K. Upadhyay, A. Palanisami, R. N. Louie, and R. A. Buhrman, "Probing ferromagnets with andreev reflection," *Physical Review Letters*, vol. 81, no. 15, pp. 3247–3250, 1998.
- [6] Y. Ji, G. J. Strijkers, F. Y. Yang, et al., "Determination of the spin polarization of half-metallic  $\text{CrO}_2$  by point contact Andreev reflection," *Physical Review Letters*, vol. 86, no. 24, pp. 5585–5588, 2001.
- [7] G. J. Strijkers, Y. Ji, F. Y. Yang, C. L. Chien, and J. M. Byers, "Andreev reflections at metal/superconductor point contacts: measurement and analysis," *Physical Review B*, vol. 63, no. 10, Article ID 104510, 6 pages, 2001.
- [8] J. G. Braden, J. S. Parker, P. Xiong, S. H. Chun, and N. Samarth, "Direct measurement of the spin polarization of the magnetic semiconductor  $(\text{Ga},\text{Mn})\text{As}$ ," *Physical Review Letters*, vol. 91, no. 5, Article ID 056602, 4 pages, 2003.
- [9] R. P. Panguluri, B. Nadgorny, T. Wojtowicz, W. L. Lim, X. Liu, and J. K. Furdyna, "Measurement of spin polarization by Andreev reflection in ferromagnetic  $\text{In}_{1-x}\text{Mn}_x\text{Sb}$  epilayers," *Applied Physics Letters*, vol. 84, no. 24, pp. 4947–4949, 2004.
- [10] R. P. Panguluri, B. Nadgorny, T. Wojtowicz, X. Liu, and J. K. Furdyna, "Inelastic scattering and spin polarization in dilute magnetic semiconductor  $(\text{Ga},\text{Mn})\text{Sb}$ ," *Applied Physics Letters*, vol. 91, no. 25, Article ID 252502, 3 pages, 2007.
- [11] H. Ohno, "Making nonmagnetic semiconductors ferromagnetic," *Science*, vol. 281, no. 5379, pp. 951–956, 1998.
- [12] T. Jungwirth, J. Sinova, J. Mašek, J. Kučera, and A. H. MacDonald, "Theory of ferromagnetic  $(\text{III},\text{Mn})\text{V}$  semiconductors," *Reviews of Modern Physics*, vol. 78, no. 3, Article ID 809, 56 pages, 2006.
- [13] L. M. Smith, T. Gurung, S. Mackowski, H. E. Jackson, G. Karczewski, and J. Kossut, "Magnetization imaging of single  $\text{CdMnTe}/\text{ZnTe}$  quantum dots," in *Proceedings of Quantum Electronics and Laser Science Conference (QELS '05)*, vol. 2, pp. 1059–1060, Baltimore, Md, USA, May 2005.
- [14] A. Haury, A. Wasiela, A. Arnoult, et al., "Observation of a ferromagnetic transition induced by two-dimensional hole gas in modulation-doped  $\text{CdMnTe}$  quantum wells," *Physical Review Letters*, vol. 79, no. 3, pp. 511–514, 1997.
- [15] M. Tanaka, "Epitaxial growth and properties of III-V magnetic semiconductor  $(\text{GaMn})\text{As}$  and its heterostructures," *Journal of Vacuum Science and Technology B*, vol. 16, no. 4, pp. 2267–2274, 1998.
- [16] R. M. Abolfath, A. G. Petukhov, and I. Žutić, "Piezomagnetic quantum dots," *Physical Review Letters*, vol. 101, no. 20, Article ID 207202, 4 pages, 2008.
- [17] R. M. Abolfath, P. Hawrylak, and I. Žutić, "Tailoring magnetism in quantum dots," *Physical Review Letters*, vol. 98, no. 20, Article ID 207203, 4 pages, 2007.
- [18] I. Žutić, J. Fabian, and S. D. Sarma, "Spintronics: fundamentals and applications," *Reviews of Modern Physics*, vol. 76, no. 2, pp. 323–410, 2004.
- [19] A. G. Petukhov, I. Žutić, and S. C. Erwin, "Thermodynamics of carrier-mediated magnetism in semiconductors," *Physical Review Letters*, vol. 99, no. 25, Article ID 257202, 4 pages, 2007.
- [20] J. K. Furdyna, "Diluted magnetic semiconductors," *Journal of Applied Physics*, vol. 64, no. 4, pp. R29–R64, 1988.

- [21] A. A. Dremin, D. R. Yakovlev, A. A. Sirenko, et al., “Electron cyclotron mass in undoped CdTe/CdMnTe quantum wells,” *Physical Review B*, vol. 72, no. 19, Article ID 195337, 5 pages, 2005.
- [22] T. Fukumura, H. Toyosaki, and Y. Yamada, “Magnetic oxide semiconductors,” *Semiconductor Science and Technology*, vol. 20, no. 4, pp. S103–S111, 2005.
- [23] T. Fukumura, Y. Yamada, H. Toyosaki, T. Hasegawa, H. Koinuma, and M. Kawasaki, “Exploration of oxide-based diluted magnetic semiconductors toward transparent spintronics,” *Applied Surface Science*, vol. 223, no. 1–3, pp. 62–67, 2004.
- [24] N. Takahashi, K. Takabayashi, I. Souma, J. Shen, and Y. Oka, “Magnetoluminescence in quantum dots and quantum wires of II-VI diluted magnetic semiconductors,” *Journal of Applied Physics*, vol. 87, no. 9, pp. 6469–6471, 2000.
- [25] I. P. Smorchkova, F. S. Flack, N. Samarth, J. M. Kikkawa, S. A. Crooker, and D. D. Awschalom, “Spin transport and optically-probed coherence in magnetic semiconductor heterostructures,” *Physica B*, vol. 249–251, pp. 676–684, 1998.
- [26] T. Kasuya and A. Yanase, “Anomalous transport phenomena in eu-chalcogenide alloys,” *Reviews of Modern Physics*, vol. 40, no. 4, pp. 684–696, 1968.
- [27] J. A. Gaj, R. Planel, and G. Fishman, “Relation of magneto-optical properties of free excitons to spin alignment of  $Mn^{2+}$  ions in  $Cd_{1-x}Mn_xTe$ ,” *Solid State Communications*, vol. 29, no. 5, pp. 435–438, 1979.
- [28] T. Hayashi, M. Tanaka, and A. Asamitsu, “Tunneling magnetoresistance of a GaMnAs-based double barrier ferromagnetic tunnel junction,” *Journal of Applied Physics*, vol. 87, no. 9, pp. 4673–4675, 2000.
- [29] K. Gnanasekar and K. Navaneethkrishnan, “Spin polaron in a quantum dot of the diluted magnetic semiconductors,” *Modern Physics Letters B*, vol. 18, no. 10, pp. 419–426, 2004.
- [30] K. Chang and F. M. Peeters, “Spin-polarized ballistic transport in diluted magnetic semiconductor quantum wire systems,” *Physical Review B*, vol. 68, no. 20, Article ID 205320, 5 pages, 2003.
- [31] C. Simserides, “Spin-subband populations and spin polarization of quasi-two-dimensional carriers under an in-plane magnetic field,” *Physical Review B*, vol. 75, no. 19, Article ID 195344, 7 pages, 2007.
- [32] Sr. Gerardin Jayam and K. Navaneethkrishnan, “Optical properties of acceptors in semimagnetic quantum well systems,” *International Journal of Modern Physics B*, vol. 16, no. 25, pp. 3737–3757, 2002.
- [33] G. Mackh, W. Ossau, D. R. Yakovlev, et al., “Localized exciton magnetic polarons in  $Cd_{1-x}Mn_xTe$ ,” *Physical Review B*, vol. 49, no. 15, pp. 10248–10258, 1994.
- [34] A. O. Govorov, “Optical probing of the spin state of a single magnetic impurity in a self-assembled quantum dot,” *Physical Review B*, vol. 70, no. 3, Article ID 035321, 5 pages, 2004.
- [35] C. Simserides and I. Galanakis, “Quasi-two-dimensional carriers in dilute-magnetic-semiconductor quantum wells under in-plane magnetic field,” *Physica E*, vol. 40, no. 5, pp. 1214–1216, 2008.

## Special Issue on 1D Nanomaterials

### Call for Papers

Nanotechnology has had a significant global impact in redefining existing and developing novel research avenues over the last two decades. Where bottom-up assembly meets conventional top-down refinements, nanomaterials proffer the necessary bridge between atomistic processes and useable macroscale devices. Focus has largely been toward preparative methods with specific interest in controlling the fundamental properties and architecture, where the inextricable link between size and geometry and properties of one-dimensional (1D) nanomaterials, for example, nanotubes, nanowires, nanorods, reveals a wide variety of promising applications. However, only a small number of nanomaterial-based devices are currently available in the market place.

The main focus of this issue will be on the development, use, and exploitation of 1D nanomaterial systems as well as their incorporation into larger devices. The special issue will become an international medium for researchers to summarize their most recent developments and ideas in the field. The topics to be covered include, but are not limited to:

- 1D nanomaterial production of inorganic and organic systems
- 1D nanomaterials and biological hybrids
- Theoretical modeling of 1D nanomaterial properties
- Functionality on the nanoscale or from the nanoscale to the macroscale
- Fabrication and/or assembly of 1D nanomaterials into macroscale devices
- New techniques for imaging and manipulation of 1D nanomaterials
- Engineering applications of 1D nanomaterials

Before submission authors should carefully read over the journal's Author Guidelines, which are located at <http://www.hindawi.com/journals/jnm/guidelines.html>. Prospective authors should submit an electronic copy of their complete manuscript through the journal Manuscript Tracking System at <http://mts.hindawi.com/> according to the following timetable:

Manuscript Due	November 1, 2009
First Round of Reviews	February 1, 2010
Publication Date	May 1, 2010

### Lead Guest Editor

**Yanqiu Zhu**, Department of Mechanical, Materials and Manufacturing Engineering, The University of Nottingham, Nottingham NG7 2RD, UK; [yanqiu.zhu@nottingham.ac.uk](mailto:yanqiu.zhu@nottingham.ac.uk)

### Guest Editors

**Raymond Whitby**, School of Pharmacy and Biomolecular Sciences, University of Brighton, Brighton BN2 4GJ, UK; [r.whitby@brighton.ac.uk](mailto:r.whitby@brighton.ac.uk)

**Renzhi Ma**, International Center for Materials Nanoarchitectonics (MANA), National Institute for Materials Science, Tsukuba, Japan; [ma.renzhi@nims.go.jp](mailto:ma.renzhi@nims.go.jp)

**Steve Acquah**, Department of Chemistry and Biochemistry, Florida State University, Tallahassee, FL 32306-4390, USA; [sacquah@chem.fsu.edu](mailto:sacquah@chem.fsu.edu)



## Special Issue on Nanomaterials for Cancer Diagnosis and Therapy

### Call for Papers

Integration of nanotechnology into the treatment of various diseases such as cancers represents a mainstream in the current and future research due to the limitations of traditional clinical diagnosis and therapy. The early detection of cancer has been universally accepted to be essential for treatment. However, it remains challenging to detect tumors at an early stage. For instance, the goal of molecular imaging in breast cancer is to diagnose the tumor with approximately 100–1000 cells, compared to the traditional techniques which may require more than a million cells for accurate clinical diagnosis. On another hand, anticancer drugs are designed to simply kill cancer cells, and their entrance into healthy organs or tissues is undesirable due to the severe side effects. In addition, the rapid and widespread distribution of anticancer drugs into nontargeted organs and tissues requires a lot of drugs with high cost. These difficulties have largely limited the successful therapy of cancer.

Nanomaterials are anticipated to revolutionize the cancer diagnosis and therapy. The development of multifunctional polymeric nanoparticles allows for the early detection of cancers. The construction of intelligent polymeric nanosystems can be used as controlled delivery vehicles to improve the therapy efficiency of anticancer drugs, that is, such vehicles are capable of delivering drugs to predetermined locations and then releasing them with preprogrammed rates in response to the changes of environmental conditions such as pH and temperature. Besides polymers, these nanomaterials can also be composed of supraparamagnetic iron oxide, carbon nanotube, metallic nanoshell, core-shell aggregate, or composites. These nanomaterials represent new directions for more effective drug administration in cancer.

This special issue of the Journal of Nanomaterials will cover a wide range of nanomaterials for cancer diagnosis and therapy. It will mainly focus on the preparations, characterizations, functionalizations, and properties of nanoparticles, nanostructured coatings, films, membranes, nanoporous materials, nanocomposites, and biomedical devices. Fundamental understanding of the basic mechanisms on material and biological processes related to the unique nanoscale properties of the materials will be the highlights of this special issue.

Papers are solicited in, but not limited to, the following areas:

- Synthesis and functionalization of polymer nanoparticle/nanomicelle/nanocomplex
- Polymer nanoparticle/hydrogel for drug delivery
- Synthesis of intelligent nanogel
- Hydrogel in nanoscale sensing
- Supraparamagnetic nanoparticle for magnetic resonance imaging applications
- Carbon nanotube-based devices for drug delivery
- Core-shell nanoparticle for molecular imaging
- Metallic nanoshell for drug delivery
- Nanoporous and nanoscaled materials for drug delivery
- Nanotechnologies for targeted delivery
- Controlled drug-delivery nanovehicles
- Biopolymers for drug/gene delivery and therapy
- Injectable hydrogels for tissue regenerations
- Bionanoparticles and their biomedical applications
- Nanomaterials for biosensors
- Toxicology of nanomaterials

Before submission authors should carefully read over the journal's Author Guidelines, which are located at <http://www.hindawi.com/journals/jnm/guidelines.html>. Prospective authors should submit an electronic copy of their complete manuscript through the journal Manuscript Tracking System at <http://mts.hindawi.com/> according to the following timetable:

Manuscript Due	October 1, 2009
First Round of Reviews	January 1, 2010
Publication Date	April 1, 2010

#### Lead Guest Editor

**Huisheng Peng**, Laboratory of Advanced Materials, Department of Macromolecular Science, Fudan University, Shanghai 200438, China; penghs2004@yahoo.com

#### Guest Editor

**Chao Lin**, The Institute for Advanced Materials and Nano Biomedicine, Tongji University, Shanghai 200092, China; chaolin@tongji.edu.cn

## Special Issue on Polymer Nanocomposite Processing, Characterization, and Applications

### Call for Papers

Polymers reinforced with nanoparticles, such as carbon nanotubes, are of great interest due to their remarkable mechanical, thermal, chemical properties as well as optical, electronic, and magnetic applications. In the general research area of polymer nanocomposites, a number of critical issues need to be addressed before the full potential of polymer nanocomposites can actually be realized. While a number of advances have recently been made in the area of polymer nanocomposites, the studies on understanding of the effects of processing parameters on the structure, morphology, and functional properties of polymer nanocomposites are deficient. There is a need for characterization techniques to quantify the concentration and distributions of nanoparticles as well as to assess the strength at the interface between the polymer and nanoparticles. Also, there is a need for the development of better models able to predict the mechanical properties of the polymer nanocomposites as functions of myriad factors including nanoparticle orientation, the type of functional groups, and the molecular weight of polymer chain. The relationships between the structural distributions and the ultimate properties of the polymer nanocomposites also need to be elucidated.

This special issue of the Journal of Nanomaterials will be devoted to emerging polymer nanocomposite processing techniques and call for new contributions in the field of characterization and applications of multifunctional nanocomposites. It intends to cover the entire range of basic and applied materials research focusing on rheological characterization, nanoparticle dispersion, and functional properties of polymer nanocomposites for sensors, actuators, and other applications. Fundamental understanding of the effects of processing and nanoparticles on the polymer structure and morphology, their optical, electrical, and mechanical properties as well as novel functions and applications of nanocomposite materials will be the highlights of this special issue.

Papers are solicited in, but not limited to, the following areas:

- Solution and melt processing of polymer nanocomposites
- Rheological and thermal characterization of nanocomposites

- Generation of nanofibers using extrusion and electrospinning of nanocomposites
- Processing-induced orientation of nanoparticles
- Quantification of nanoparticle dispersion
- Effect of nanoparticle incorporation on polymerization
- In situ nanoparticle formation in polymer matrix
- Noncovalent functionalization techniques and characterization of properties at polymer-nanoparticle interface
- Novel applications of polymer nanocomposites

Before submission authors should carefully read over the journal's Author Guidelines, which are located at <http://www.hindawi.com/journals/jnm/guidelines.html>. Prospective authors should submit an electronic copy of their complete manuscript through the journal Manuscript Tracking System at <http://mts.hindawi.com/> according to the following timetable:

Manuscript Due	November 1, 2009
First Round of Reviews	February 1, 2010
Publication Date	May 1, 2010

#### Lead Guest Editor

**Gaurav Mago**, Lubrizol Advanced Materials, Inc., Avon Lake, OH 44141, USA; [gaurav.mago@lubrizol.com](mailto:gaurav.mago@lubrizol.com)

#### Guest Editors

**Dilhan M. Kalyon**, Highly Filled Materials Institute, Department of Chemical Engineering and Materials Science, Stevens Institute of Technology, Hoboken, NJ, USA; [dilhan.kalyon@stevens.edu](mailto:dilhan.kalyon@stevens.edu)

**Sadhan C. Jana**, Department of Polymer Engineering, University of Akron, Akron, OH, USA; [janas@uakron.edu](mailto:janas@uakron.edu)

**Frank T. Fisher**, Department of Mechanical Engineering, Stevens Institute of Technology, Hoboken, NJ, USA; [frank.fisher@stevens.edu](mailto:frank.fisher@stevens.edu)